# Quantum Information Propagation and Scrambling

Gabriel Perko-Engel

## Contents

# 1 Introduction

The field of quantum scrambling and chaos is both immensely vast and profoundly deep. It touches topics as distant as the whether information can be reconstructed after being radiated from a black hole [1]. But, at the same time, ot addresses how information is dispersed across a phase transition in condensed matter systems like the Bose-Hubbard model [2]. The open questions in the field are similarly expansive. For example, while it is known that that fast scrambling is a necessary condition black hole duality, the question of whether it's a sufficient condition has not yet completely solved [3]. And while the study of scrambling in thermal states has been investigated deeply, much more work is needed to identify bounds on scrambling time in non-thermal states [3].

Given the vastness of the discipline, I cannot hope to cover it all in this paper. Nevertheless, I attempt motivate some intuition for how information disperses in quantum systems with a series of simulations. I then explore a number of tools and protocols that can be used to further characterize quantum scrambling and check for it experimentially. One particular case of experimental verification on a seven qubit quantum computer is fleshed out in more detail. Nevertheless, there are many important characterizations and limits on quantum chaos such as the Lyapunov exponent and Lieb-Robinson bounds that I don't have the chance to even touch on [4]. The curious reader is encouraged to use the examples and sources presented here as a jumping off point to delve into this topic in greater detail.

# 2 Technical Content and Discussion

## 2.1 Dispersion of Quantum Information

I'd first like to motivate the idea and methods of scrambling by getting a sense of how information can propagate through a many body quantum system. Perhaps the simplest of these to work with is the one dimensional mixed field Ising model.[1]. Consider a chain of spin qubits at fixed and equally separated points. It has open (non-periodic) boundary conditions so that

[1]This computation was inspired by a similiar, but more limited, example here [4]

I may act on one end of the chain and see how my action propagates out through the rest of the chain. The hamiltonian to describe such a system is

$$H = -J \sum_{r=1}^{N-1} \sigma_r^z \sigma_{r+1}^z - h_z \sum_r \sigma_r^z - h_x \sum_r \sigma_r^x. \tag{1}$$

Here $J$ is the nearest-neighbor coupling energy. When the $h_z$ free parameters is set to zero, the chain becomes a model of non-interacting fermions in one dimension. I set $J = h_z = h_x = 1$ in my simulatinos.

We now define a reference qubit $R$ that the Hamiltonian doesn't act on and is a copy of the first qubit's initial state. That way, as the system evolves, we can compare the reference with some other part of the chain to see how the information initially held in the first qubit has moved around. To this end, we split the chain into two subsystems $A$ and $B$. $A$ is the subsystem we'll compare with the reference and $B$ just contains the rest of the chain. It's now time to set up the state of the first qubit.

Let $|\psi_1\rangle_{AB} = |1, 1, \cdots, 1\rangle_{AB}$ be the state of chain with all spin-up qubits. And let the orthogonal state $|\psi_2\rangle_{AB} = |0, 1, \cdots, 1\rangle_{AB}$ be the state with only the first qubit down. The two states differ only by acting the operator $W = \sigma_1^x$ on this qubit. We now entangle the first qubit with the reference in an EPR pair to prepare the initial state of the system.

$$|\psi\rangle_{ABR} = \frac{1}{\sqrt{2}} \left( |\psi_1\rangle_{AB} |1\rangle_R + |\psi_2\rangle_{AB} |0\rangle_R \right) \tag{2}$$

The density matrix corresponding to this state is $\rho^{ABR} = |\psi\rangle_{ABR} \langle\psi|_{ABR}$. We can then evolve this state in time and extract the relevant subsystems as needed. We use units where $\hbar = k_B = 1$ from here on out.

$$\rho^{ABR}(t) = U^\dagger(t) \rho^{ABR} U(t), \quad \text{where } U(t) = e^{-iHt} \tag{3}$$

To find the mutual information between $A$ and $R$, we care about these two subsystems as well as their union. The states of these subsystems can be attained by taking the partial trace over

all other subsystems.

$$\begin{aligned} \rho^A(t) &= \mathrm{tr}_{BR}\left[\rho^{ABR}(t)\right] \\ \rho^R(t) &= \mathrm{tr}_{AB}\left[\rho^{ABR}(t)\right] \\ \rho^{AR}(t) &= \mathrm{tr}_{B}\left[\rho^{ABR}(t)\right] \end{aligned} \tag{4}$$

The von Neumann entropy of these subsystems is then found like so.

$$\begin{aligned} S(A) &= -\,\mathrm{tr}\left[\rho^A(t)\log_2\left(\rho^A(t)\right)\right] \\ S(R) &= -\,\mathrm{tr}\left[\rho^R(t)\log_2\left(\rho^R(t)\right)\right] \\ S(A,R) &= -\,\mathrm{tr}\left[\rho^{AR}(t)\log_2\left(\rho^{AR}(t)\right)\right] \end{aligned} \tag{5}$$

And from here, we can get the mutual information of $A$ and $R$ [5, 6].

$$I(A:R) = S(A) + S(R) - S(A,R) \tag{6}$$

Now that our model is completely established. It's time to simulate the Ising chain and watch the information move around. The computation is described in more detail in appendix B. The simulated results of an $N = 4$ qubit Ising chain are shown in figure 1. Since only the first qubit is initially entangled with the reference qubit, the two bits of information about the starting condition are contained entirely within this site. But, as time progresses, the information rapidly disperses. There's an early spike in the second qubit, then the third, and fourth as the information propagates down the chain. Given how short the chain is, the information quickly gets to and saturates the fourth site and washes back to the first in a somewhat periodic manner. But, over time, the information eventually gets dispersed more or less evenly between all the sites. This is the point where the information has become scrambled. The effects of this are more apparent in the longer chain of figure 2.

A more intuitive way to understand the "speed" at which the information propogates is to look at when it leaves a certain region. To this end, I've run a similar simulation between the

reference $R$ and the first $n$ qubits of an $N = 9$ qubit chain.

$$A(n) = \{\text{first } n \text{ qubits of the chain}\} \tag{7}$$

The results of this simulation are shown in figure 3. We can take the first inflection point on each of the curves shown as the time when the information leaves a given $A(n)$ region. And we can let $\Delta t$ be the apparent constant spacing between them. This is the time difference between when information leaves qubit $n$ and when it leaves qubit $n+1$. Now let $\Delta r$ be the spacing between the sites the qubits sit at on the Ising lattice. Then, for given interaction strengths $J, h_x, h_z$ between the sites, we have an information velocity $v = \Delta r/\Delta t$. The bound on how quickly information can propogate through a system is called the butterfly velocity $v_B$ and is better defined in the context of out-of-time-ordered-correlators (OTOCs).[2] In the case of information scrambling within a black hole and being scattered outwards, it is natural to take the speed of light $c$ as the butterfly velocity [1, 3, 4].

### 2.2 Signs of Scrambling: OTOCs

Many systems with interesting scrambling dynamics exist in a mixed thermal state $\rho$ dependent on the temperature of the environment they're in. From statistical mechanics, we have that a system in thermal equilibrium at temperature $T = 1/\beta$ starts out as

$$\rho = \frac{e^{-\beta H}}{Z} = \sum_n \frac{e^{-\beta E_n}}{Z} |n\rangle\langle n| \tag{8}$$

with $H$ being the hamiltonian for the system and $Z = \text{tr}\left[e^{-\beta H}\right]$ the partition function. Now say we have two non-conserved *local* operators $W(r)$ and $V(r')$ acting on the system at sites $r$ and $r'$ respectively. And say the systems takes some relaxation tiem $\tau$ to retern to a local thermal equilibrium after it is slightly perturbed. A simple example would be an Ising chain like the one considered earlier, but with the spins distributed thermally rather than all prepared in the spin-up state [3, 7]. If we were to perturb the system such that a small local cluster

[2] Although I explain OTOCs in greater detail in short order, I do not expand on the butterfly velocity. See the cited sources for a more in depth overview.

(centered at site $r$) of qubits were all set to the same spin state then the relaxation time would be the time for time for the system to thermalize and for the information in the perturbation to get scattered throughout the system.

Now lets think about how we might measure this dispersion. We can choose $W(r)$ and $V(r')$ to be operators that approximately commute for an $r$ and $r'$ that are far apart from each other. But as the information from the perturbation spreads from site $r$ to site $r'$, the operators can be chosen such that the commutators of $W(r)$ and $V(r')$ start to diverge. However, thermalization is characterized by the effective loss of information. So, given a long enough time $t \gg \tau$ and that the system sufficiently thermalizes, the information will be lost from site $r$ and so the time evolved version of $W(r)$ approximately-commute with with the initial $V(r')$ to the same degree. This can be stated more precisely like so.

$$\big\langle [W(r,t), V(r')] \big\rangle = \mathrm{tr}\left[\frac{e^{-\beta H}}{Z}[W(r,t), V(r')]\right] \approx 0 \quad \text{when } t \gg \tau \tag{9}$$

The out-of-time-ordered-correlator (OTOC) $F(t)$ is one of the primary tools used to measure the "overlap" between these final states and therefore to characterize the dispersion of information to many degrees of freedom.

$$F(t) = \left\langle W^\dagger(t) V^\dagger W(t) V \right\rangle \tag{10}$$

The utility comes from the relationship between the OTOC and the hermitian square of the commutator for unitary $W$ and $V$ [3].

$$C(t) = \left\langle |[W(t), V]|^2 \right\rangle = 2(1 - \mathrm{Re}[F(t)]) \tag{11}$$

If $W$ and $V$ are not unitary, then the commutator's square has other non-constant time-ordered correlators. We explore some ways around this difficulty in section 2.4.

For a hamiltonian that scrambles information (such as a sufficiently long and periodic Ising chain), the square commutator's magnitude is offset by a small–but persistent–real part of $F(t)$ [3]. The time scale $t_*$ where $C(t)$ becomes significant is called the scrambling time [7].

But if the hamiltonian is non-scrambling, $W$ and $V$ may diverge for a short time. However, the information will not remain scattered through other degrees of freedom in the system. So, it will eventually return and allow $W$ and $V$ to approximately commute once more.

To show this happening, I explicitly compute the real OTOC for a particle in a box with $W = x$ and $V = p$.[3] First, I prepare the oscillator in the thermal state $\rho$ then evolve it in time and measure the square correlator using the identity

$$C(t) = \frac{1}{Z}\sum_n e^{-\beta E_n}\left|\sum_k \frac{ix_{nk}x_{km}}{2}\left(\delta E_{km}e^{i\delta E_{nk}} - \delta E_{nk}e^{i\delta E_{km}}\right)\right|^2. \tag{12}$$

I derive this identity in appendix A. Note that $\delta E_{nm} = E_n - E_m$.

The infinite eigenvalues of the particle in a box mean I need to cut off the energies considered at some maximum value $k_c$. Luckily, the energies don't all contribute equally. Setting $m = 1$, the partition function is as follows.

$$Z = \mathrm{tr}\left[e^{-\beta H}\right] = \sum_{k=1}^{\infty} e^{-\beta\pi^2 k^2/2} = \sum_{k=1}^{\infty} r^{k^2} = \frac{\vartheta_3(0,r) - 1}{2} \tag{13}$$

Where $r = e^{-\beta\pi^2/2}$, $\vartheta_3$ is the Jacobi elliptic theta function, and I have plugged in the energy solutions $E_k = k^2\pi^2/2$ for a particle in a box ($\hbar$ is still set to unity). Note that $r^{k^2}$ is small for large $\beta\pi^2k^2/2 = \pi^2k^2/2T$. That is to say that

$$\frac{\pi^2k^2}{2} \gg T \implies k \gg \frac{\sqrt{2T}}{\pi}. \tag{14}$$

So, the contributions to the sum are exponentially suppressed for $k$ greater than this value. In my computations I include up to the smallest $k$ value greater than this cutoff with the understanding that that term is already suppressed because of the square. I drop all terms after this cutoff $k_c$.

$$k_c = \frac{\sqrt{2T}}{\pi} + 1 \tag{15}$$

[3]The same OTOC can actually be solved analytically for a harmonic oscillator. In that case, it's a perfect sinusoidal curve periodic in the oscillator's frequency $\omega$ [8].

And experimentially, I've found that including still higher terms really does make negligable difference. The effects of not including sufficiently high terms are on display in figure 4.

A more interesting observation is the periodicity of the OTOC in figure 5. Given the simplicity of our non-scrambling and single-body hamiltonian, the information from our momentum "perturbation" disperses briefly through the system's degrees of freedom. But, it coalesces back to its initial state before it can have a chance to thermalize. Also of note is the OTOC's changing structure as the temperature increases. In the low temperature ($T \approx 0$) OTOC of figure 6 there is a much more complex shape than in the high temperature ($T = 200$) case shown in figure 7. Since the OTOC's shape is increasingly sharp and linear at higher temperatures, it seems reasonable to conclude that the structure is due to the discreteness of the energy levels. At low temperature, the quadratic difference between energies of the particle in a box dominate and make the path of information more "circuitous" through this region. But, at high temperatures, the low energy contributions are much more negligable. And since the higher energy levels approach each other exponentially, they can be treated as approximately continuous and the information can propagate through them linearly.[4] However, in all cases, the non-scrambling nature of the hamiltonian still emerges and the system returns to its original state in the same period.

## 2.3 Measuring OTOCs

Given the utility of OTOCs in describing how "chaotic" a quantum system is, several protocols have been developed for measuring the OTOC in an experimental setting. I identify two relatively simple "system agnostic" protocols here that can be adapted to a broad array of quantum computer architectures [9].

### 2.3.1 Interferometric Protocol

The main idea of ther interferometric protocol is to prepare a reference qubit $R$ that you carefully entangle with the system $S$ such that the OTOC is an observable you can measure

[4] It's worth noting that previous calculations of these OTOCs have been more "bulbous" than the ones I've found [8]. I'm not sure what the cause of this discrepency is.

from $R$ directly. The reference qubit is first prepared in the $|+X\rangle_R$ state $(|0\rangle_R+|1\rangle_R)/\sqrt{2}$. The reference is then entangled with the system's unperturbed state and state as acted on with the time chosen time independent observable $V_S$. Letting $\mathbf{1}$ be the identity operator, this is akin to acting on the state with the gate

$$\mathbf{1}_S \otimes |0\rangle\langle 0|_C + V_S \otimes |1\rangle\langle 1|_C \,. \tag{16}$$

The other time evolved operator is then applied to system by acting on it with the following gate sequence.

$$\begin{aligned} 1: &\quad U(t)_S \quad \otimes \quad \mathbf{1}_C \\ 2: &\quad W_S \quad \otimes \quad \mathbf{1}_C \\ 3: &\quad U^\dagger(t)_S \quad \otimes \quad \mathbf{1}_C \end{aligned} \tag{17}$$

Finally, the opposite ordering of the initial gate is applied to the system as well.

$$V_S \otimes |0\rangle\langle 0|_C + \mathbf{1}_S \otimes |1\rangle\langle 1|_C \tag{18}$$

This leaves the complete $SR$ system system in the final state

$$\frac{(VW(t)\,|\psi\rangle)_S\,|0\rangle_C + (W(t)V\,|\psi\rangle)_S\,|1\rangle_C}{\sqrt{2}} \tag{19}$$

regardless of the initial state $|\psi\rangle_S$ of the system. The real and imaginary parts of the OTOC can then just be extracted by measuring $R$ in the $\sigma_x$ and $\sigma_y$ bases.

$$F(t) = \langle\sigma_x\rangle + i\,\langle\sigma_y\rangle \tag{20}$$

### 2.3.2 Distinguishability Protocol

In cases where a reference qubit is unavailable, the distinguishability protocol allows you to measure $|F(t)|^2$. While this isn't the OTOC exactly, it has roughly the same time scales and therefore still captures much of the same physics. The protocol is also very simple conceptually.

You just apply the OTOC operators to the initial state $|\psi_i\rangle$.

$$|\psi_f\rangle = W^\dagger(t)V^\dagger W(t)V\,|\psi_i\rangle \tag{21}$$

And then you measure the final state $|\psi_f\rangle$ acted on with the projector $\Pi = |\psi_i\rangle\langle\psi_i|$.

Although the distinguishability protocol is apparently very simple, it requires that the initial state be known and easy enough to implement $\Pi$ with. This leaves many interesting problems potentially infeasible to address in this way.

### 2.4 Decoherence and the Problems with OTOCs

Despite the theoretical appeal of OTOCs, their difficulty goes beyond the feasability of implementing decoding protocols. Once again, we consider the OTOC's long run behavior.

$$F(t) = \left\langle W^\dagger(t)V^\dagger W(t)V \right\rangle \tag{22}$$

If scrambling occurs with time, then $W(t)$ becomes increasingly nonlocal. This causes the OTOC to decay and allows measurement of the OTOC to be taken as a sign of scrambling. But, non-unitary time evolution due to classical noise and depolarization can cause the OTOC to decay independent of quantum scrambling. Likewise, a small inconsistency between the forwards and backwards time evolution of $W$ can also cause the OTOC to decay. To this end, there has been some effort to develop and implement teleportation protocols that can confirm the existence of scrambling without relying on measuring the OTOC.

One such protocol has been experimentally verified on a seven qubit quantum computer at the University of Maryland. The protocol takes inspiration from the black hole information paradox mentioned earlier [1, 10, 11]. The idea is to simulate the "black hole" with a unitary circuit $U$ that's manually built to maximally scramble any input it could receive. Since black holes are assumed to be the fastest scramblers in nature, the time scale of the of the scrambling can be treated as instantaneous [12]. Therefore, the whole process can be done by merely acting once with the scrambling operator.

The actual goal of the experiment is to simulate someone (Alice) throwing a secret quantum state $|\psi\rangle$ into the black hole and seeing if the scrambled information can still be decoded from the emitted "Hawking radiation" by an outside observer (Bob) on the other side (represented by the scrambler's complex conjugate $U^*$) of a two-sided black hole (a wormhole).

Bob is assumed to have access to two "memory" qubits that are part of EPR pairs that have been previously entangled with the black hole. This is reasonable as Bob could have prepared some entangled qubits before casting them into the black hole himself. These EPR pairs make up the wormhole itself and therefore are also the qubits radiated out. Bob also has access to half of an ancillary EPR pair $|\phi\rangle$ which is the be the recipient of Alice's teleported state.

If $U$ is properly designed to be maximally scrambling, then information encoded in $|\psi\rangle$ is immediately distributed throughout the EPR pairs that make up the black hole and should therefore be emitted as hawking radiation and also accessible in Bob's memory qubits. From there, he can do projective measurements between his memory qubits and the corresponding radiated qubits to reconstruct $|\phi\rangle$ into $|\psi\rangle$ if the black hole unitary is indeed maximally scrambling. Otherwise, $|\phi\rangle$ will not quite equal the $|\psi\rangle$ that Alice initially threw in.

More explicitly, the initial state of the system (before any teleportation or scrambling) is

$$|\Phi_i\rangle = 2^{-3/2}\,|\psi\rangle_1\,(|0\rangle_2\,|0\rangle_5 + |1\rangle_2\,|1\rangle_5)\,(|0\rangle_3\,|0\rangle_4 + |1\rangle_3\,|1\rangle_4)(|0\rangle_6\,|0\rangle_7 + |1\rangle_6\,|1\rangle_7). \tag{23}$$

The first two terms in the parentheses are the entangled memory and the to-be-radiation qubits that make up the black hole. The last term in the parentheses is Bob's ancilla EPR pair of which the qubit $|\phi\rangle_7$ will ultimately have Alice's qubit $|\psi\rangle_1$ teleported to it. We then apply the scrambling operator $U$ to the black hole qubits that are radiated and the decoding operator $U^*$ to the corresponding memory qubits to get the final state $|\Phi_f\rangle$ of the system.

$$|\Phi_f\rangle = \underbrace{(\mathbf{1}_{1,2,3} \otimes U^*_{4,5,6} \otimes \mathbf{1}_7)}_{\text{decoding}}\underbrace{(U_{1,2,3} \otimes \mathbf{1}_{5,6,7,8})}_{\text{scrambling}}\,|\Phi_i\rangle \tag{24}$$

We can also write this state out explicitly. I drop the constant factor.

$$\begin{aligned}
|\Phi_f\rangle = \quad & (U|\psi\rangle_1|0\rangle_2|0\rangle_3)(U^*|0\rangle_4|0\rangle_5|0\rangle_6)|0\rangle_7 + (U|\psi\rangle_1|1\rangle_2|0\rangle_3)(U^*|0\rangle_4|1\rangle_5|0\rangle_6)|0\rangle_7 \\
& + (U|\psi\rangle_1|0\rangle_2|1\rangle_3)(U^*|1\rangle_4|0\rangle_5|0\rangle_6)|0\rangle_7 + (U|\psi\rangle_1|1\rangle_2|1\rangle_3)(U^*|1\rangle_4|1\rangle_5|0\rangle_6)|0\rangle_7 \\
& + (U|\psi\rangle_1|0\rangle_2|0\rangle_3)(U^*|0\rangle_4|0\rangle_5|1\rangle_6)|1\rangle_7 + (U|\psi\rangle_1|1\rangle_2|0\rangle_3)(U^*|0\rangle_4|1\rangle_5|1\rangle_6)|1\rangle_7 \\
& + (U|\psi\rangle_1|0\rangle_2|1\rangle_3)(U^*|1\rangle_4|0\rangle_5|1\rangle_6)|1\rangle_7 + (U \underbrace{|\psi\rangle_1}_{\text{Alice's}} \underbrace{|1\rangle_2|1\rangle_3}_{\text{radiated}})(U^* \underbrace{|1\rangle_4|1\rangle_5}_{\text{memory}} \underbrace{|1\rangle_6)|1\rangle_7}_{\text{ancilla}}
\end{aligned} \tag{25}$$

This is the state that Bob ends up with before doing any projections. For clarity, I have shown which qubits are radiated, which were in memory, and which are Bob's ancilla qubits. He has access to all of these qubits but does not to the qubit which Alice threw in. Now Bob applies projective measurements to the pairs $(2,5)$ and $(3,4)$ which were the original EPR pairs from equation 23. If $U$ is maximally scrambling, then it disperses all single-qubit operators into three-qubit operators. If $\sigma_i$ is the Pauli operator for $i \in \{x, y, z\}$ then this means that

$$\begin{aligned}
U^\dagger(\sigma_i \otimes \mathbf{1} \otimes \mathbf{1})U &= \sigma_i \otimes \sigma_k \otimes \sigma_k \\
U^\dagger(\mathbf{1} \otimes \sigma_i \otimes \mathbf{1})U &= \sigma_k \otimes \sigma_i \otimes \sigma_k \\
U^\dagger(\mathbf{1} \otimes \mathbf{1} \otimes \sigma_i)U &= \sigma_k \otimes \sigma_k \otimes \sigma_i
\end{aligned} \tag{26}$$

where $i$, $j$, and $k$ are an ordered index of the Pauli operators. Therefore, if $U$ is maximally scrambling, then the teleportation protocol will be successful. In general, the probability of a successful projective measurement $P_\psi$ is directly related to the OTOC when ignoring decoherence and errors. Let $V = |\psi\rangle\langle\phi|$ act on Alice's qubit and $W(t)$ be the local projective measurement on the Hawking radiated qubits. The time $t$ determines whether we are before or after scrambling. Letting $\int d\phi \int dW$ be the average over Bob's single qubit states and the the local unitaries Bob could use, an exact form for $P_\psi$ can be given [10].

$$P_\psi = \int d\phi \int dW \left\langle W^\dagger(t)V^\dagger W(t)V \right\rangle \tag{27}$$

This equation is still valid when allowing for noise and dephasing. But, $U(t)$ is no longer the

scrambling unitary operator. However, the fidelity $F_\psi = |\langle\phi|\psi\rangle|^2$ of the teleportation can still be tested over many runs of the protocol for numerous initial states of $|\psi\rangle$. This allows for an OTOC-independent method of determining the extent of scrambling as well as a means to determing the error-induced decay caused by classical noise.

## 3 Conclusion

The examples presented here are just the very edge of the vast world of quantum chaos. I've demonstrated basic characteristics of how information propogates through several incredibly simple quantum systems. But, the real world is not quite so easy to pin down and solve explicitly. Indeed, even the jump from one to two body simulations like the stadium billiard display much more complex behavior than what I've shown here [8]. However, the basic tools, methods, and protocols I've used in this paper are applicable to a much broader set of systems. But, this is still only the beginning. Already, incredible similarities have been found between a broad set of systems ranging from condensed matter, to quantum computing, to the limits of quantum gravity. In the last year alone, huge progress has been made towards finding a solution to the black hold information paradox [13]. The quest to classify and understand quantum chaos is ongoing and certain to reveal new fascinating new insights in the years to come.

# A Derivation of OTOC for Particle in a Box

The OTOC is defined as $F(t) = \left\langle W^\dagger(t)V^\dagger W(t)V \right\rangle$ and its real part appears prominantly in the square commutator $C(t)$ as described in section 2.2. For the "particle in a box" case, we have $W = x$ and $V = p$ being observed over a thermal state.

$$\begin{aligned} C(t) &= -\left\langle [x(t), p(0)]^2 \right\rangle \\ &= -\operatorname{tr}\left[ [x(t), p(0))]^2 \rho \right] \\ &= -\operatorname{tr}\left[ [x(t), p(0))]^2 \sum_n \frac{e^{-\beta E_n}}{Z} |n\rangle\langle n| \right] \\ &= -\sum_n \frac{e^{-\beta E_n}}{Z} \operatorname{tr}\left[ [x(t), p(0)]^2 |n\rangle\langle n| \right] \\ &= -\sum_n \frac{e^{-\beta E_n}}{Z} \langle n| [x(t), p(0)]^2 |n\rangle \end{aligned} \tag{28}$$

Let the term sandwiched between the bra and ket be $c_n$. We can expand and simplify it like so.

$$\begin{aligned} c_n &= \langle n| [x(t), p(0)]^2 |n\rangle \\ &= \langle n| (x(t)p(0) - p(0)x(t))^2 |n\rangle \\ &= \langle n| (x(t)p(0) - p(0)x(t)) \left( \sum_m |m\rangle\langle m| \right) (x(t)p(0) - p(0)x(t)) |n\rangle \\ &= -\sum_m |(x(t)p(0) - p(0)x(t)) |m\rangle|^2 \\ &= -\sum_m |b_{nm}|^2 \end{aligned} \tag{29}$$

Where $b_{nm}$ is the following.

$$\begin{aligned} b_{nm} &= \langle n| \left(x(t)p(0) - p(0)x(t)\right) |m\rangle \\ &= \langle n| x(t) \left(\sum_k |k\rangle\langle k|\right) p(0) |m\rangle - \langle n| p(0) \left(\sum_k |k\rangle\langle k|\right) x(t) |m\rangle \\ &= \sum_k \langle n| U^\dagger x U |k\rangle\langle k| p |m\rangle - \langle n| p |k\rangle\langle k| U^\dagger x U |m\rangle \\ &= \sum_k e^{i(E_n - E_k)t} x_{nk} p_{km} - e^{i(E_k - E_m)t} p_{nk} x_{km} \end{aligned} \tag{30}$$

We've acted with the unitaries on the left and right states. And $p_{nm}$ and $x_{nm}$ are the matrix elements of the momentum and position operators at $t = 0$. We now consider many body hamiltonians of the following form.

$$H = \sum_{i=1}^{N} p_i^2 + V(x_1, \cdots, x_N) \tag{31}$$

And for cases where the position and potential commute this simplifies quite nicely.

$$\begin{aligned} [H, x_j] &= \left[\sum_i p_i^2, x_j\right] \\ &= \left[\sum_{i=1}^{N} p_i^2, x_j\right] + [V(x_1, \cdots, x_N), x_j] \\ &= \left[\sum_{i=1}^{N} p_i^2, x_j\right] \\ &= \sum_i p_i[p_i, x_j] + [p_i, x_j]p_i \\ &= \sum_i -p_i \delta_{ij} i\hbar - \delta_{ij} i\hbar p_i \\ &= -2ip_j \end{aligned} \tag{32}$$

We can use this to extract the position and momentum matrix elements.

$$\begin{aligned} -2i \langle n| p_j |m\rangle &= \langle n| [H, x_j] |m\rangle \\ &= \langle n| Hx_j |m\rangle - \langle n| x_j H |m\rangle \\ &= (E_n - E_m) \langle n| x_j |m\rangle \\ \implies p_{nm} &= \frac{i(E_n - E_m)}{2} x_{nm} \end{aligned} \tag{33}$$

Letting $\delta E_{nm} = E_n - E_m$ we can plug this into $b_{nm}$ to get the result used earlier.

$$\begin{aligned} b_{nm} &= \sum_k e^{\delta E_{nk}} \frac{i\delta E_{km}}{2} x_{nk} x_{km} - e^{\delta E_{km}} \frac{i\delta E_{nk}}{2} x_{nk} x_{km} \\ &= \sum_k \frac{i x_{nk} x_{km}}{2} \left( \delta E_{km} e^{i\delta E_{nk}} - \delta E_{nk} e^{i\delta E_{km}} \right) \end{aligned} \tag{34}$$

And now we just stick this back into our OTOC to get the identity used in the computation.

$$C(t) = \frac{1}{Z} \sum_n e^{-\beta E_n} \left| \sum_k \frac{i x_{nk} x_{km}}{2} \left( \delta E_{km} e^{i\delta E_{nk}} - \delta E_{nk} e^{i\delta E_{km}} \right) \right|^2 \tag{35}$$

# B Computations for Ising Chain and Particle in a Box

I have published all the code I used in both of this paper's simulations in GitHub hosted repository at `https://github.com/GabePoel/Quantum-Information-Propagation`. The file `box_otoc.py` contains the code for all the OTOC simulations of a particle in a box and `ising_info.py` has the code for the Ising chain simulations. No quantum computation libraries were used. Instead, I elected to construct the vector spaces with `numpy` and `scipy` explicitly using a series of Kronecker tensor products. This means the hamiltonian for the Ising chain is put together by building the operators for each term in the sum and summing

over them. For example, the 4-qubit hamiltonian is

$$\begin{aligned} H_4 = &- \sigma_1^z \otimes \sigma_2^z \otimes \mathbf{1}_3 \otimes \mathbf{1}_4 - \mathbf{1}_1 \otimes \sigma_2^z \otimes \sigma_3^z \otimes \mathbf{1}_4 - \mathbf{1}_1 \otimes \mathbf{1}_2 \otimes \sigma_3^z \otimes \sigma_4^z \\ &- h_z \left(\sigma_1^z \otimes \mathbf{1}_{2,3,4} + \mathbf{1}_1 \otimes \sigma_2^z \otimes \mathbf{1}_{3,4} + \mathbf{1}_{1,2} \otimes \sigma_3^z \otimes \mathbf{1}_4 + \mathbf{1}_{1,2,3} \otimes \sigma_4^z\right) \\ &- h_x \left(\sigma_1^x \otimes \mathbf{1}_{2,3,4} + \mathbf{1}_1 \otimes \sigma_2^x \otimes \mathbf{1}_{3,4} + \mathbf{1}_{1,2} \otimes \sigma_3^x \otimes \mathbf{1}_4 + \mathbf{1}_{1,2,3} \otimes \sigma_4^x\right). \end{aligned} \tag{36}$$

The spin states were created similarly with Kronecker products over the one-qubit state for each link in the chain. In the examples shown, I computed the non-integrable interacting Ising chain for $J = h_x = h_z = 1$.

Due to limited computing power, the largest Ising chain I solved for was only nine qubits long. Given the growth of the vector space with each Kronecker product, the overall runtime of the algorithms is $\mathcal{O}(2^N)$ where $N$ is the number of qubits in the chain. So, each additional qubit I added more or less doubled the computation time. All the code has multiprocessing support to account for this a little. But still, an actual quantum computer would be needed to run a *real* simulation of information propagation on a long Ising chain in a computationally feasible way.

The OTOC computations are much faster as they grow at order $\mathcal{O}(k_C^2)$ where $k_C$ is the cutoff energy level described earlier. The quadratic runtime comes from the necesity of determining each element of a $k_C$ by $k_C$ matrix. Thanks to the identity derived in appendix A, I can avoid multiplying the matrices out and keep the runtime relatively low.

## C Figures

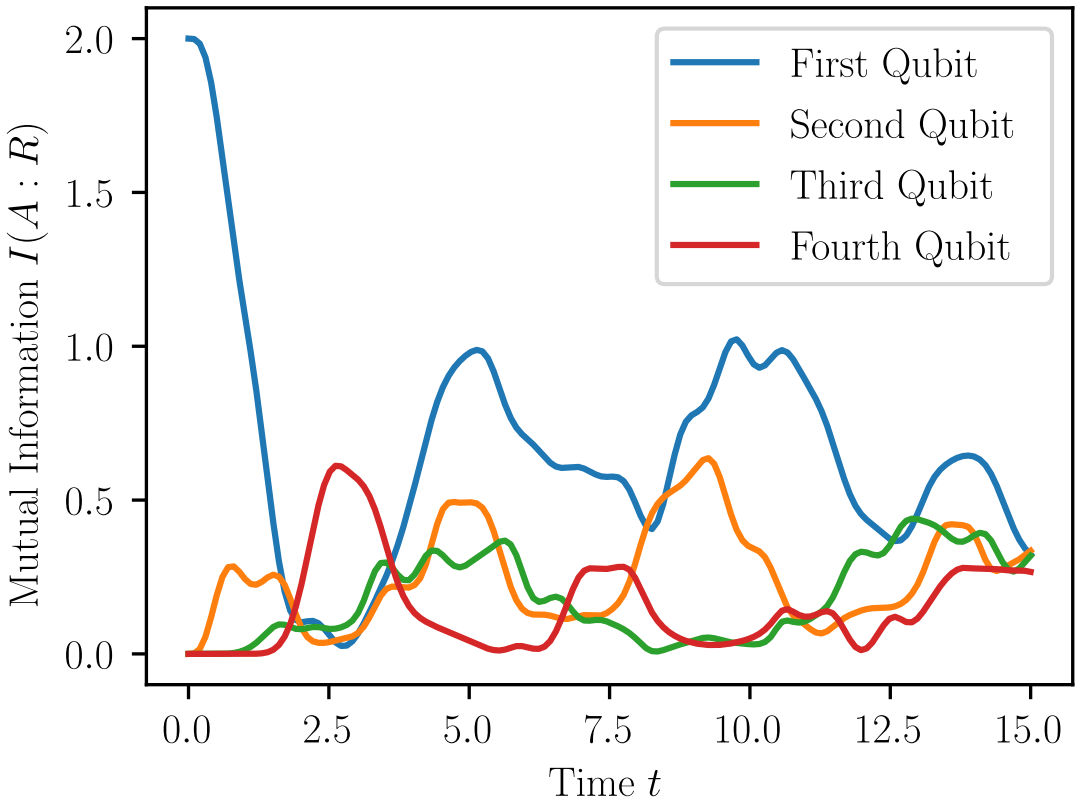


Figure 1: The mutual information between the reference qubit $R$ and each of the qubits in a four qubit chain as a function of time. Initially both bits of information are found only in the first qubit. But, under the evolution of the hamiltonian, the information rapidly spreads to the second, then third, and fourth qubit where it briefly builds up before sloshing back into the first one. Although the propagation of the information through the chain isn't truly periodic, the time scale at which it moves around appears to be. The motion between the qubits can be more easily seen in the nine qubit chain of figure 2.

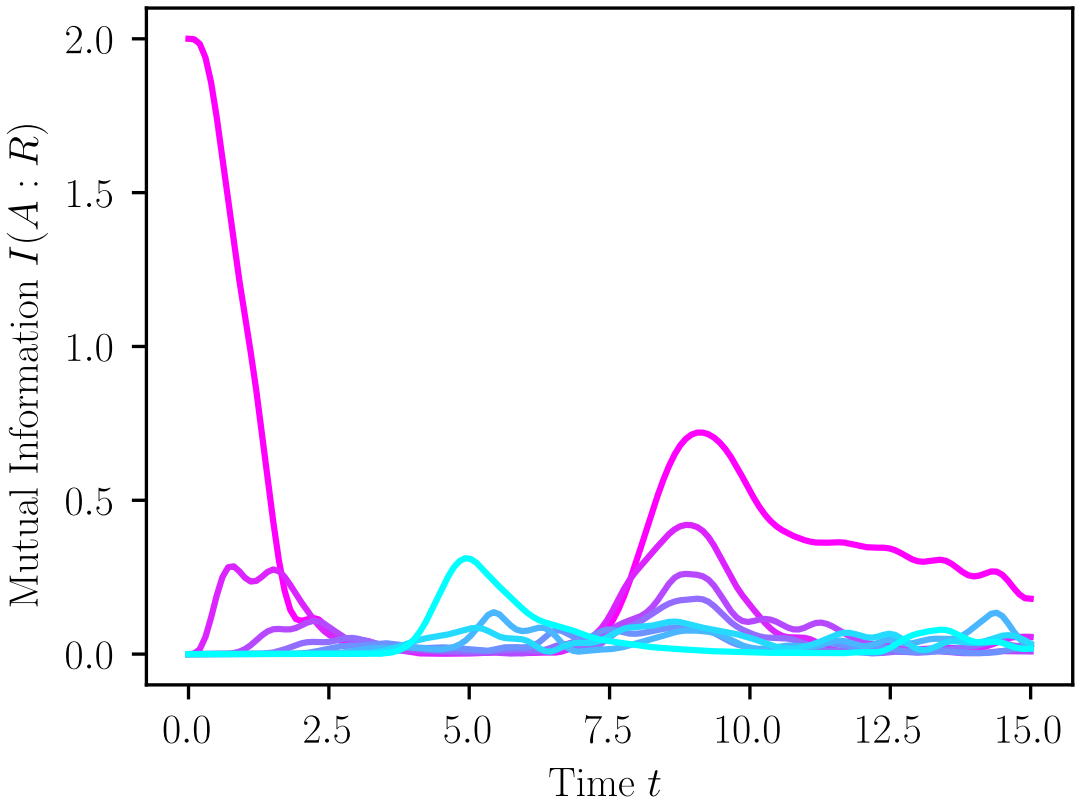


Figure 2: The mutual information between the reference qubit and each other one in a nine qubit Ising chain. The more pink the curve is, the earlier in the chain the qubit it corresponds to is. We can see that as the chain gets longer the appearance of periodicity gets much less pronounced. The time scale to reach and build up upon the last qubit in the chain appears to be propartional to the length of the chain. But, after hitting the last qubit, the information reflects off the first one once more before appearing to more or less decay from this state and scatter throughout the rest of the chain.

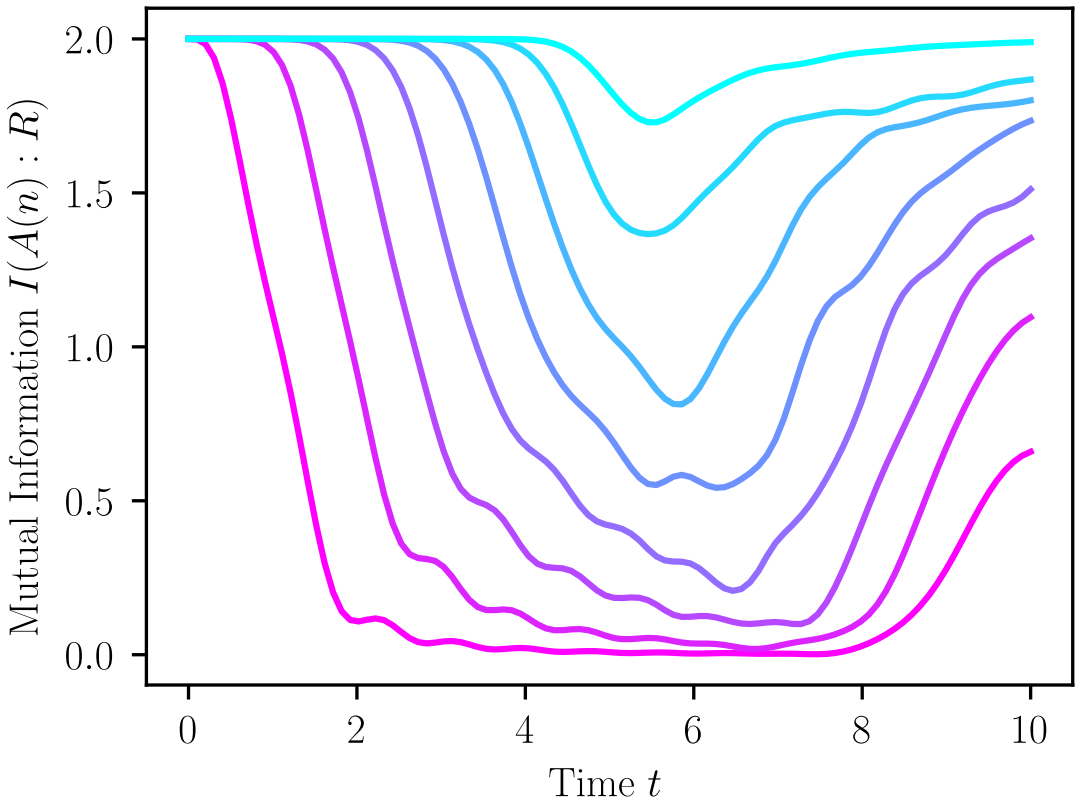


Figure 3: The mutual information between the reference $R$ and the first $n$ qubits $A(n)$ on a nine qubit chain. The pinkest curve is for $A(1)$ and the most cyan curve is for $A(8)$. The evenly spaced inflection points denote when the information starts to leave the $A(n)$ region. By dividing $\Delta r$ by the time spacing between these we get the velocity that information travels through the chain as bound by the butterfly velocity $v_B$.

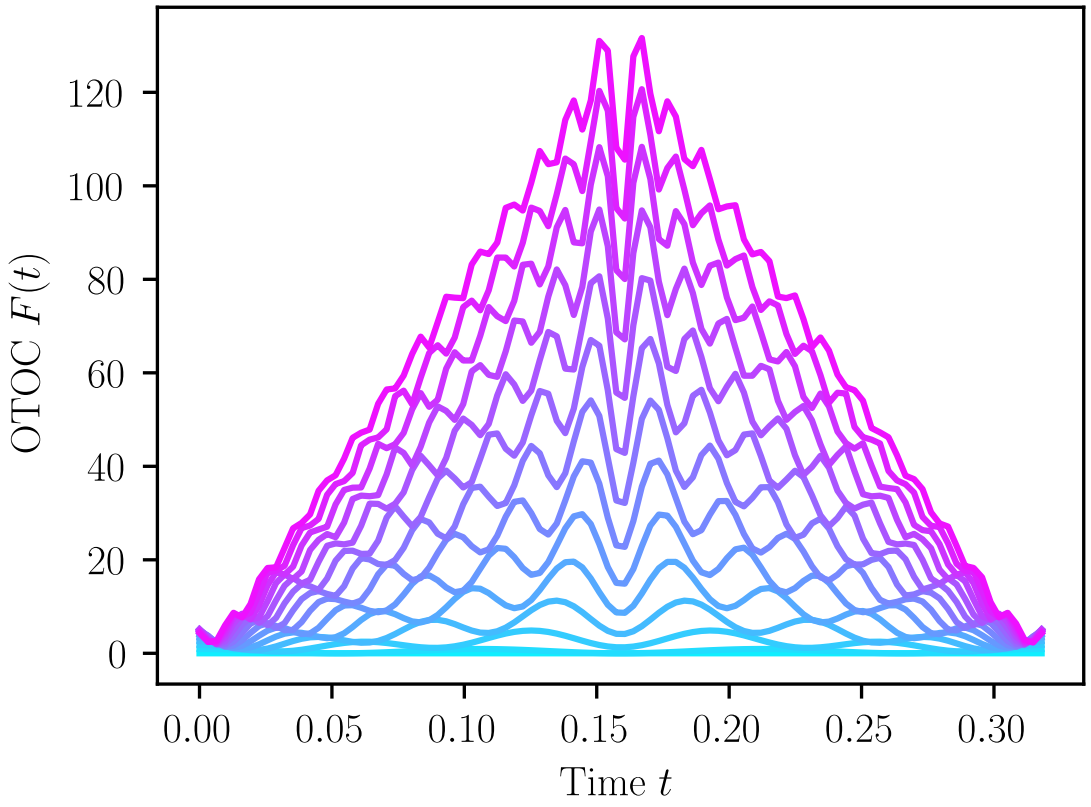


Figure 4: The OTOC for a particle in a box calculated for $T = 1000$ with only the first 15 energy levels included. Although the general pyramid shape can still be observed, the higher frequency terms do not yet converge to the actual shape of the OTOC. The cyan curves are calculated with a lower cutoff energy and the pink ones are higher.

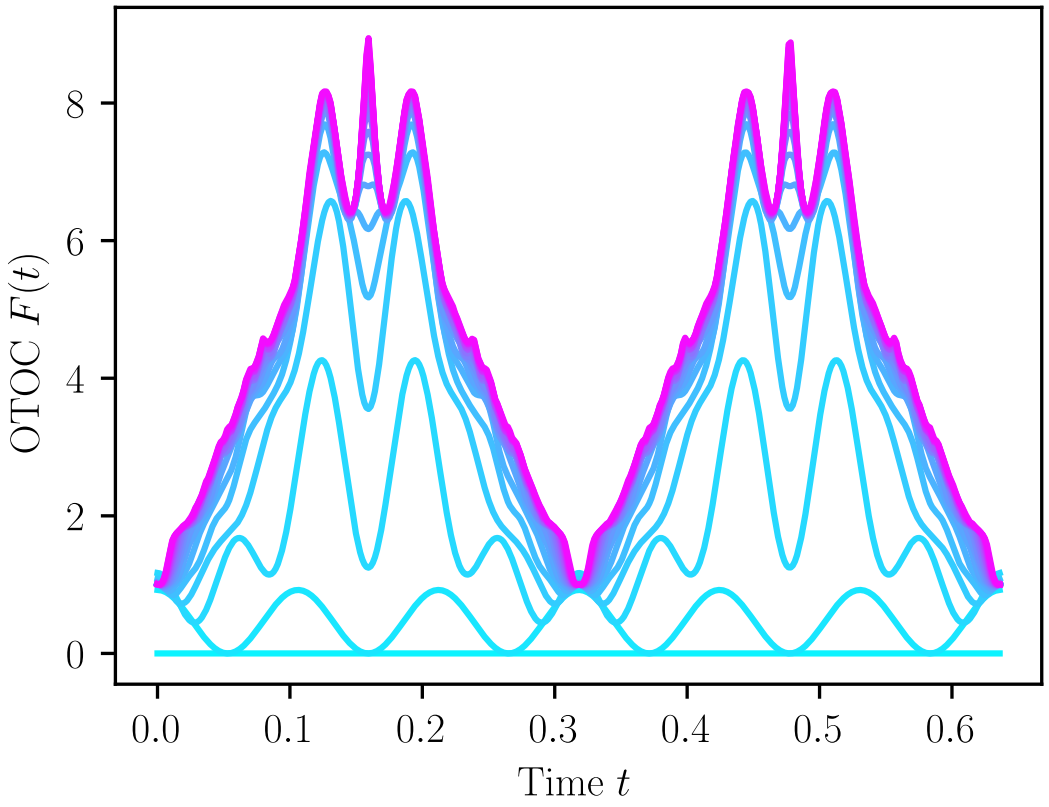


Figure 5: A semi-low temperature ($T = 20$) particle in a box OTOC. The structure is periodic in time due to the simple single-body non-scrambling hamiltonian.

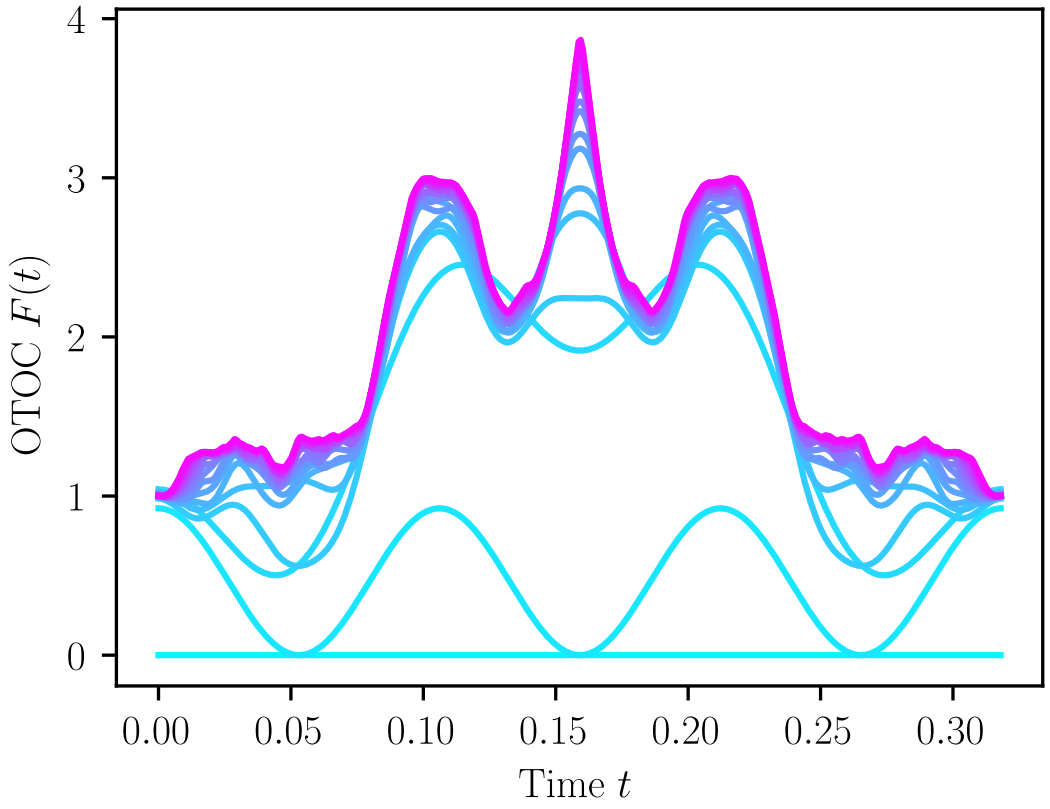


Figure 6: The particle in the box OTOC computed for $T \approx 0$. The structure is most interesting at low temperature as the information is unable to quickly disperse through the system's degrees of freedom before returning to its initial state. As such, the quadratic difference between the energy levels may dominate the geometry of the curve that emerges. At low temperatures, the high frequency terms clearly converge rather quickly. The main contribution from higher frequencies is to add more "texture" to the shape of the OTOC.

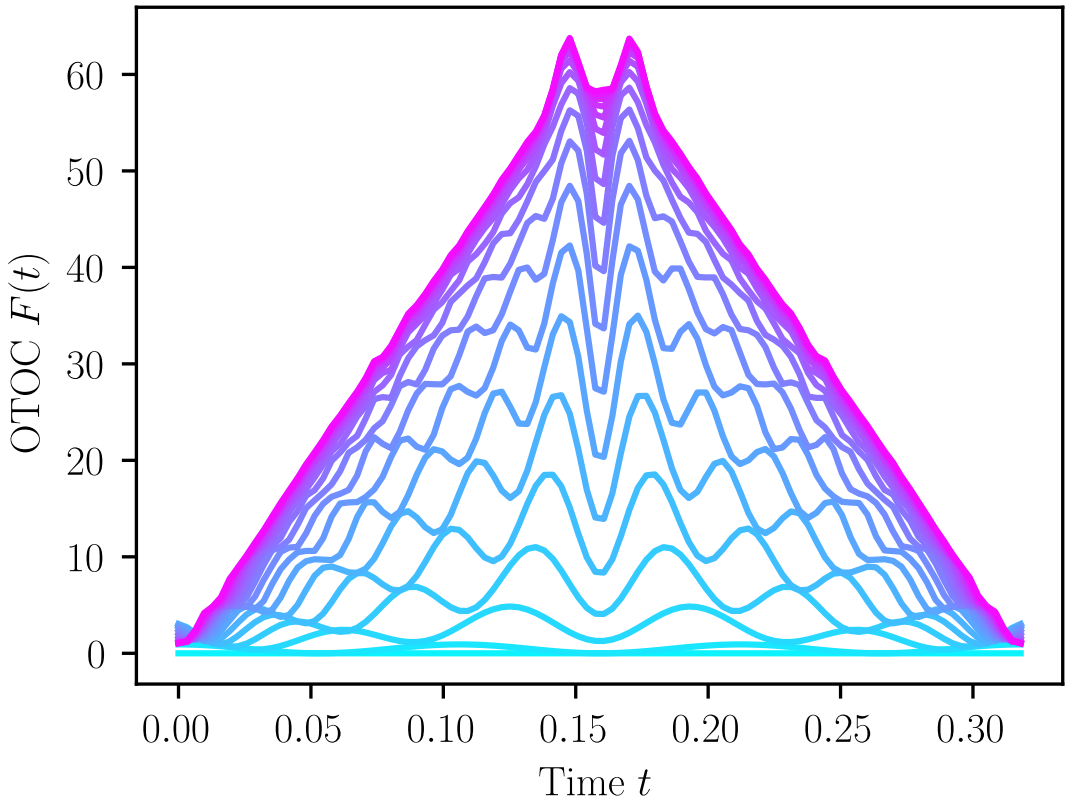


Figure 7: OTOC computer at $T = 200$. At high temperatures, the OTOC converges to a *slightly* bulbous horned pyramid shape. This could be because at high temperatures differences in energy levels is negligable so the information can treat them as if they were continuous and move linearly through them.

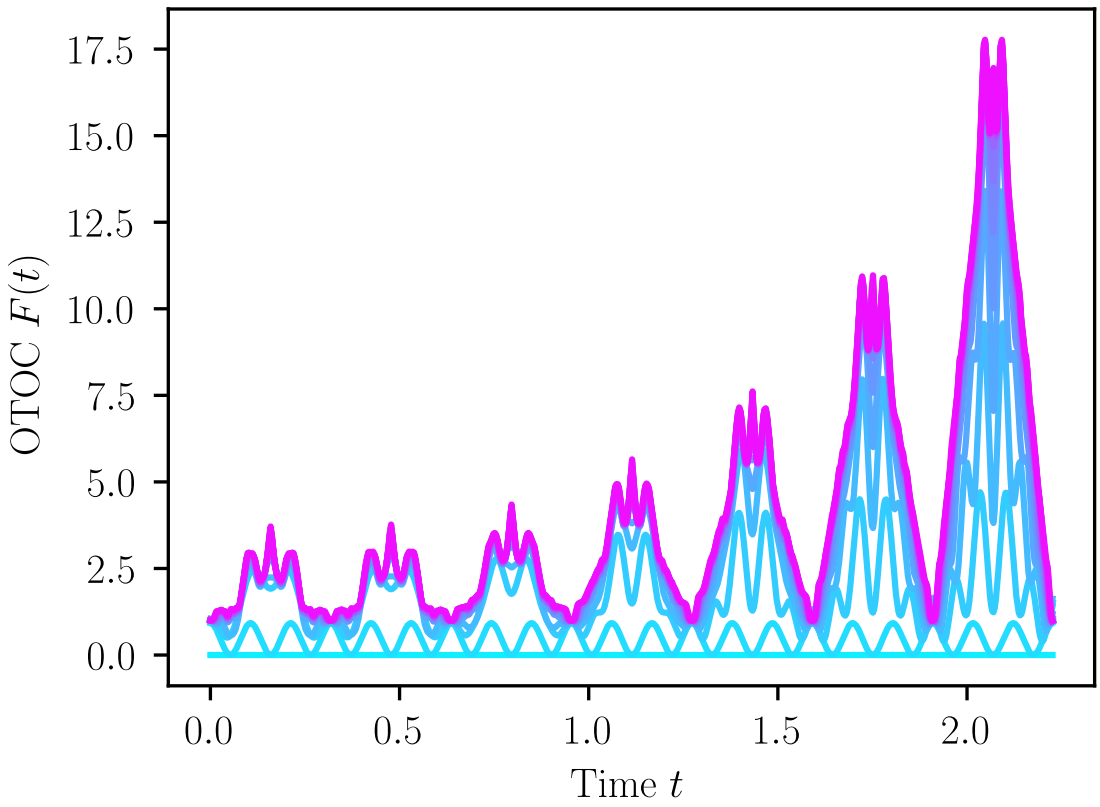


Figure 8: The OTOC calculated at many different temperatures. The cycle on the far left is calculated at $T = 1$ and each following is done at twice the temperature of one preceeding it. At a little after $T = 30$ there's a turning point where the peak of the OTOC is no longer halfway through its period, but slightly before and after. This is shown by the "horns" topping the pyramid on the right. At even higher temperatures, the horns seem to get closer to each other. The other loss in structure at higher temperatures is also shown by the increasingly triangular shape of the OTOCs. The rising heights of the OTOCs also demonstrates the increased rate of dispersion of information at higher temperatures.

# D References


[1] Leonard Susskind and Ying Zhao. Teleportation through the wormhole. *Physical Review D*, 2018.

[2] Huitao Shen, Pengfei Zhang, Ruihua Fan, and Hui Zhai. Out-of-time-order correlation at a quantum phase transition. *Physical Review B*, 2016.

[3] José Raúl González Alonso, Nicole Yunger Halpern, and Justin Dressel. Out-of-time-ordered-correlator quasiprobabilities robustly witness scrambling. *Physical Review Letters*, 2019.

[4] Brian Swingle. Quantum information scrambling: Boulder lectures. `https://boulderschool.yale.edu/sites/default/files/files/qi_boulder.pdf`, 2018.

[5] Thomas Cover and Joy Thomas. *Elements of Information Theory*. 2006.

[6] Isaac Chuang and Michael Nielsen. *Quantum Computation and Quantum Information*. 2000.

[7] Juan Maldacena, Stephen Shenker, and Douglas Stanford. A bound on chaos. *Journal of High Energy Physics*, 2016.

[8] Koji Hashimoto and Keiju Murata. Out-of-time-order correlators in quantum mechanics. *Journal of High Energy Physics*, 2017.

[9] Brian Swingle, Gregory Bentsen, Monika Schleier-Smith, and Patrick Hayden. Measuring the scrambling of quantum information. *Physical Review A*, 2016.

[10] K. A. Landsman, C. Figgatt, T. Schuster, N. M. Linke, B. Yoshida, N. Y. Yao, and C. Monroe. Verified quantum information scrambling. *Nature*, 2019.

[11] Beni Yoshida and Norman Yao. Disentangling scrambling and decoherence via quantum teleportation. *Physical Review X*, 2019.

[12] Yasuhiro Sekino and Leonard Susskind. Fast scramblers. *Journal of High Energy Physics*, 2018.

[13] Ahmed Almheiri, Thomas Hartman, Juan Maldacena, Edgar Shaghoulian, and Amirhossein Tajdini. Replica wormholes and the entropy of hawking radiation. *Journal of High Energy Physics*, 2020.